*Optica Applicata, Vol. XLIII, No. 1, 2013*
DOI: 10.5277/oa130101

# Ohmic contacts for room-temperature AlGaAs/GaAs quantum cascade lasers (QCL)

ANNA BARAŃSKA[1*], ANNA SZERLING[1], PIOTR KARBOWNIK[1],
KRZYSZTOF HEJDUK[1], MACIEJ BUGAJSKI[1], ADAM ŁASZCZ[1],
KRYSTYNA GOŁASZEWSKA-MALEC[1], WOJCIECH FILIPOWSKI[2]

[1]Institute of Electron Technology, al. Lotników 32/46, 02-668 Warszawa, Poland

[2]Silesian University of Technology, Faculty of Automatic Control, Electronics and Computer Science, Institute of Electronics, ul. Akademicka 16, 44-100 Gliwice, Poland

[*]Corresponding author: abar@ite.waw.pl

This paper reports on the results of optimization of the ohmic contacts for GaAs/AlGaAs quantum cascade lasers (QCLs). Technological parameters during the optimization procedure concerned time and temperature of thermal processing as also the ratio of metallic layers thickness. The main goal of this work was to obtain stable ohmic contacts with low resistance and a smooth surface. Circular transmission line method (CTLM) was applied for the electrical characterization of the Ni/AuGe/Ni/Au and AuGe/Ni/Au metallization systems. Transmission electron microscopy (TEM) method was used for the characterization of microstructures. Elements concentration in layers was determined by the energy dispersive X-ray spectroscopy (EDXS). The best results for the specific contacts resistivity, thermal stability and morphology were obtained when the Ni/AuGe/Ni/Au and the AuGe/Ni/Au systems were processed at 440 °C and 400 °C, respectively.

Keywords: ohmic contacts, *n*-GaAs, CTLM, EDXS, TEM.

## 1. Introduction

The quantum cascade lasers (QCLs) are unipolar devices based on intersubband transitions and tunnelling transport [1, 2]. The GaAs-based QCLs are an effective source of laser radiation in mid-infrared (MIR) as well as far-infrared (FIR) regions. They have applications in the gas sensing systems (*e.g.*, for detecting $CO_2$, NO, $CH_4$) [2], medical diagnostics [3] and environment monitoring [4]. One of the main requirements in the ohmic contacts fabrication process is their low resistivity. It plays an important role in the serial resistivity of the final device. High quality ohmic contacts allow to achieve low threshold voltage and minimize the amount of heat generated in the laser structure. The other important ohmic contact properties are:

thermal stability, lateral uniformity of metal–semiconductor (m–s) interfaces and low depth of metal diffusion into semiconductor layers.

Contacts based on the AuGe/Ni/Au sandwich layers are extensively used for fabrication of the ohmic contacts in the *n*-type GaAs and AlGaAs/GaAs heterostructures [3, 5]. The most common approach in the formation of the AuGe-based ohmic contacts is sequential deposition of the AuGe, Ni and Au metals onto the GaAs wafer followed by annealing. During the alloying process at higher temperatures (above 365 °C), the Au, Ni and Ge start to react with GaAs and new compounds are formed. Ga atoms diffuse out from the GaAs substrate to the contact metal creating Ga vacancies, while Ge atoms diffuse from the NiAs(Ge) layer to the Ga vacancy sites, providing donors close to the metal/GaAs interface [4]. Nickel is added into the alloy as a wetting agent. The low surface tension of Ni helps to prevent the AuGe metal from "balling-up" during the alloying process as well as improves the adherence [6] and the surface morphology of the contact. Furthermore, adding a layer of Ni between the GaAs and the AuGe improves metal adhesion [7] and it is a very good diffusion barrier for gold atoms [8]. Au in AuGe alloy enhances the out-diffusion of Ga. This results in the substitution of the Ga sites with Ge and produces the desired highly doped *n*-GaAs layer [9]. However, an excess of Au or Ni can degrade the contact resistance. Apart from that, an excess of Au most likely leads to the excessive Ga out-diffusion, which leaves behind an excess of As. Au and Ni can also act as the acceptors and may compensate the donors in the underlying *n*-doped highly conductive layer [5]. During the annealing at a temperature above 420 °C, the NiAs(Ge), $\beta$-AuGa and other compound layers are formed at the interface of the contact. It was noted that values of the specific contact resistance decrease monotonically with the increase of the total area of the GaAs interface covered by NiAs(Ge) layers [4].

The aim of this work was to optimize the technology of the ohmic contacts to the *n*-type GaAs for the MIR quantum cascade lasers as well as to obtain stable ohmic contacts with low resistance and smooth surface. Two metallization systems were investigated: the Ni/AuGe/Ni/Au, which can be used on the top of the device (as a contact to epi-layers of heterostructure), and the AuGe/Ni/Au system, which can be used as a contact to the GaAs substrate. In this paper we present the results of investigations into various annealing parameters (temperature and annealing time). Furthermore we show the behavior of the AuGe/Ni/Au system versus the thickness of the Ni layer. The electrical properties and the thermal stability of the ohmic contact were correlated with their microstructure.

## 2. Experimental details

The ohmic contacts were manufactured on the wafers of *n*-type GaAs:Si doped to $2\times10^{18}$ cm$^{-3}$. Prior to the experiment, the samples received a standard surface cleaning by treatment in hot organic solvents. The ohmic contact pattern for test with the circular transmissions line method (CTLM) [10] was defined by the lift-off processes. Before the metal deposition, the patterned samples were cleaned by $Ar^+$ plasma. The metal-

lic layers Ni(5 nm)/AuGe(100 nm)/Ni(35 nm)/Au(300 nm) and AuGe(225 nm)/Ni($x$)/Au(300 nm), for $x$ = 45, 56, 60, and 75 nm, were sequentially deposited on patterned GaAs wafers by DC magnetron sputtering using the Leybold L400sp system. Finally samples were cleaned in the hot organic solvents and annealed by using the rapid thermal annealing (RTA) with continuous flow of the forming gas (67% $N_2$ + 26% Ar + + 7% $H_2$).

Time of the thermal treatment of the ohmic contacts varied from 30 to 120 s and the temperature was in the range from 400 to 440 °C. Long-term thermal stability was investigated by annealing samples in a gas flow furnace at a temperature of 150 °C for 4 h prior to the annealing at 200 °C for 8 h.

The specific resistance was determined by the CTLM method. The study of the contact surface morphology was performed with the profile measurement gauge (KLA-Tencor P-16+) and the atomic force microscope (AFM). The microstructure of the annealed (Ni/AuGe/Ni/Au, AuGe/Ni($x$)/Au) layers was observed by the transmission electron microscope (TEM) using the JEM-2100 (JEOL). The elements concentration in the layers was determined by the energy dispersive X-ray spectroscopy (EDXS) in the scanning transmission electron microscope (STEM) mode.

## 3. Results and discussion

Figure 1 shows the Ni(5 nm)/AuGe(100 nm)/Ni(35 nm)/Au(300 nm) contact deposited on the GaAs:Si. Four successive layers of Ni, AuGe, Ni and Au, which have not reacted with each other, can be observed (Fig. 1). The first thin Ni layer between AuGe and GaAs:Si improves wetting and adhesion and leads to the formation of more uniform contacts [7].

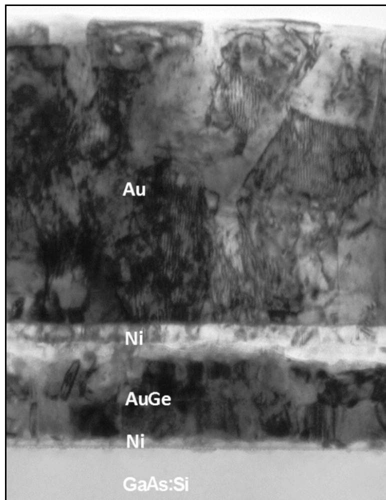


Fig. 1. TEM image of the as-deposited Ni(5 nm)/AuGe(100 nm)/Ni(35 nm)/Au(300 nm) contact deposited on GaAs:Si.

The GaAs:Si/Ni/AuGe/Ni/Au microstructure images after the annealing at 435 °C for different time intervals (30 s, 90 s, 120 s) are shown in Figs. 2**a**, 2**b** and 2**c**, respectively, while Tab. 1 presents results from the EDXS microanalysis for those samples. In this table the "major phase observed" has been identified on the basis of YIH-CHENG SHIH [7] and MURAKAMI [4] works. All samples annealed at 435 °C have the uniform layer with high density of NiAs grains containing Ge (bright area) and a small portion of a phase containing mainly Au (dark area) in the m–s interfaces (Fig. 2).

The samples annealed for 30 and 120 s, in the place of small dark areas (location A1 in Fig. 2**a**, C3 and C4 in Fig. 2**c**), contain all components of the contact in particular atoms of Au, Ni, As, Ga. They are localized between NiAs(Ge) grains. Ni, As, Ga

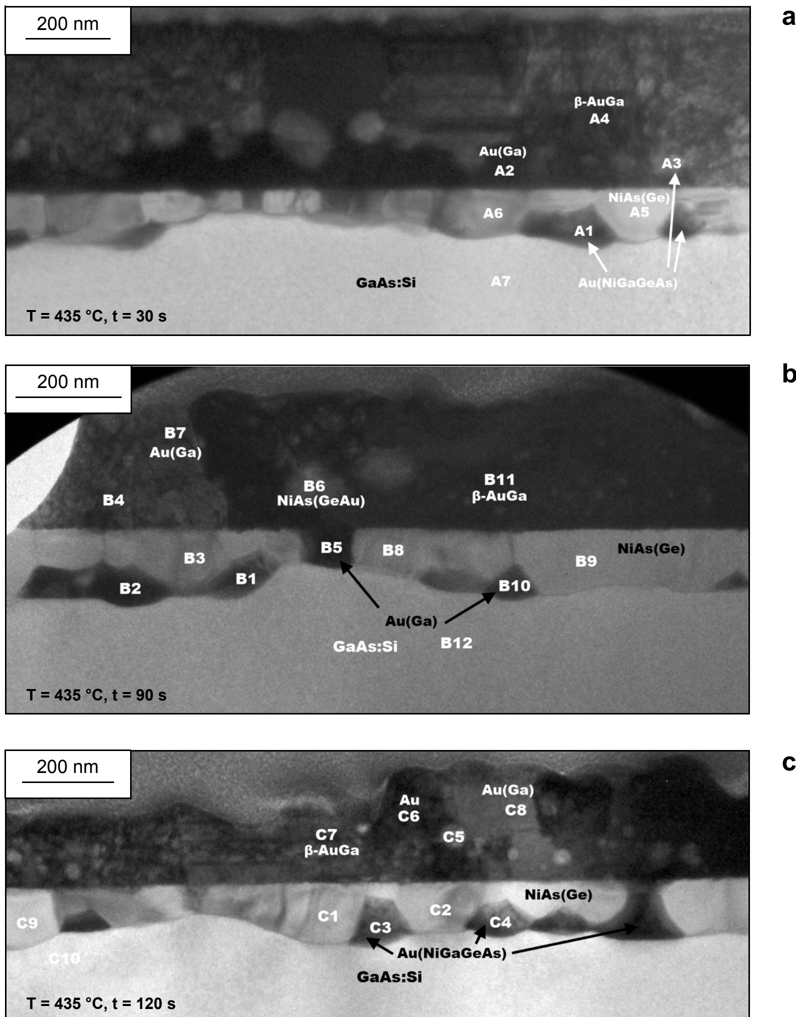


Fig. 2. TEM images of Ni(5 nm)/AuGe(100 nm)/Ni(35 nm)/Au(300 nm) ohmic contacts annealed at 435 °C for 30 s (**a**), 90 s (**b**), and 120 s (**c**).

T a b l e 1. Chemical compositions of the phase formed in Ni/AuGe/Ni/Au contacts annealing at 435 °C determined by X-ray energy dispersive spectrometry microanalysis.

| Microanalysis location | Annealing time [s] | Chemical composition [at.%] | | | | | Major phase observed |
|---|---|---|---|---|---|---|---|
| | | Ni | Ga | Ge | As | Au | |
| A1 | 30 | 30.41 | 5.3 | 8.02 | 20.27 | 36 | Poly-Au(NiGaGeAs) |
| A2 | 30 | 0 | 10.30 | 0 | 2.82 | 86.88 | Au(Ga) |
| A3 | 30 | 24.12 | 5.2 | 11.18 | 12.97 | 46.53 | Poly-Au(NiGaGeAs) |
| A4 | 30 | 0 | 11.65 | 0 | 1.84 | 86.51 | $\beta$-AuGa |
| A5 | 30 | 52.19 | 0.66 | 10.08 | 36.43 | 0.64 | NiAs(Ge) |
| A6 | 30 | 51.10 | 0.48 | 7.34 | 40.69 | 0.39 | NiAs(Ge) |
| A7 | 30 | 0 | 48 | 0 | 52 | 0 | GaAs |
| B1 | 90 | 6.08 | 10.37 | 0 | 6.7 | 76.85 | Au(Ga) |
| B2 | 90 | 1.75 | 10.33 | 0 | 4.29 | 83.63 | Au(Ga) |
| B3 | 90 | 54.62 | 0.52 | 7.09 | 37.44 | 0.33 | NiAs(Ge) |
| B4 | 90 | 0 | 8.67 | 0 | 1.83 | 89.5 | Au(Ga) |
| B5 | 90 | 3.67 | 8.54 | 0 | 4.15 | 83.64 | Au(Ga) |
| B6 | 90 | 39.13 | 1.82 | 16.85 | 20.66 | 21.54 | NiAs(Ge, Au) |
| B7 | 90 | 0 | 10.04 | 0 | 1.55 | 88.41 | Au(Ga) |
| B8 | 90 | 52.48 | 1.07 | 3.50 | 42.89 | 0.06 | NiAs(Ge) |
| B9 | 90 | 53.48 | 0.05 | 13.54 | 32.71 | 0.22 | NiAs(Ge) |
| B10 | 90 | 8.87 | 10.22 | 0 | 5.85 | 75.06 | Au(Ga) |
| B11 | 90 | 0 | 21 | 0 | 2.01 | 76.99 | $\beta$-AuGa |
| B12 | 90 | 0 | 51.1 | 0 | 48.83 | 0.07 | GaAs |
| C1 | 120 | 52.29 | 0.31 | 11.6 | 35.6 | 0.2 | NiAs(Ge) |
| C2 | 120 | 52.31 | 0.46 | 8.39 | 38.41 | 0.43 | NiAs(Ge) |
| C3 | 120 | 27.36 | 6.6 | 6.56 | 18.44 | 41.04 | Poly-Au(NiGaGeAs) |
| C4 | 120 | 18.65 | 6.99 | 5.77 | 12.04 | 56.55 | Poly-Au(NiGaGeAs) |
| C5 | 120 | 0 | 12.17 | 0 | 2.26 | 85.57 | $\beta$-AuGa |
| C6 | 120 | 0 | 2.6 | 0.17 | 3.04 | 94.19 | Au |
| C7 | 120 | 0 | 10.11 | 0 | 1.79 | 88.1 | $\beta$-AuGa |
| C8 | 120 | 0 | 9.39 | 0 | 2.04 | 88.57 | Au(Ga) |
| C9 | 120 | 52.10 | 0.14 | 13.82 | 33.57 | 0.37 | NiAs(Ge) |
| C10 | 120 | 0 | 50.18 | 0 | 49.68 | 0.14 | GaAs |

atoms could segregate at the boundaries of Au grains and prevent the grain growth, which results in the formation of small polycrystalline Au grains [7].

In contrast to the samples annealed for 90 s, these small dark areas (location B1, B2, B5, B10 in Fig. 2**b**) contain mainly Au, Ga and small amounts of Ni and As atoms. This indicates the existence of the Au(Ga) phase in this place. A dark layer (location B4, B6, B7, B11 in Fig. 2**b**) containing Au and elements such as Ga and As was formed on the top of the NiAs(Ge) layers and GaAs:Si substrate. This highest layer of contact is probably a mixture of Au, Au(Ga), $\beta$-AuGa phases and NiAs(Ge) grains. As it was

described in the literature [7], the number of NiAs(Ge) grains in the m–s interfaces has a significant impact on contact resistance $\rho_c$. The $\rho_c$ values decrease with increasing the total area of the GaAs interface covered by the NiAs(Ge) grains [4].

A growth of NiAs(Ge) grains and an increasing diffusion of the Au atoms from the upper layer at the NiAs(Ge) grain boundaries in the direction of the substrate appear with the increasing annealing time (Figs. 2**a** and 2**b**). Moreover the top layer (mixture of Au, Au(Ga), $\beta$-AuGe phase) reduces its thickness. The diffusion of Au atoms leads to the creation of long dark areas near the surface of GaAs:Si that separates it from the NiAs(Ge) phase (Fig. 2**b**). However, the EDXS chemical analysis (Table 1) of GaAs:Si substrate (locations A7, B12, C10 in Figs. 2**a** and 2**b**) does not indicate the diffusion of gold atoms into the substrate. (The result of measurement of the level of doping with gold in the area B12 and C10 is 0.07 at.% and 0.14 at.%, respectively, with EDXS chemical analysis error at 1%. So this level of gold doping could be measurement error and we suppose that the diffusion of gold into the substrate does not occur.)

The specific contact resistance measurement of samples annealed at 435 and 440 °C for different annealing times was shown in Fig. 3. Higher values of $\rho_c$ for the short and long annealing times are believed to be due to non-ideal interfacial morphology between the metal and semiconductor. For the sample annealed at 435 °C for 30 and 60 s the time was too short and metal/GaAs reaction was not completed. The reaction continued during subsequent annealing even though the temperature was lower than the ohmic contact formation temperature [4]. For samples annealed at 435 °C for 120 s and samples annealed at 440 °C for 90 and 120 s annealing interval was too long. For those samples gold reacts with GaAs forming layers containing different Au phases. This reaction caused the expansion of the area in which the Au(Ga)/GaAs interface is distinguished and the reduction in the surface of the NiAs(Ge) layers takes place. This phenomenon caused an increment of the $\rho_c$ values as it is shown in Fig. 3.

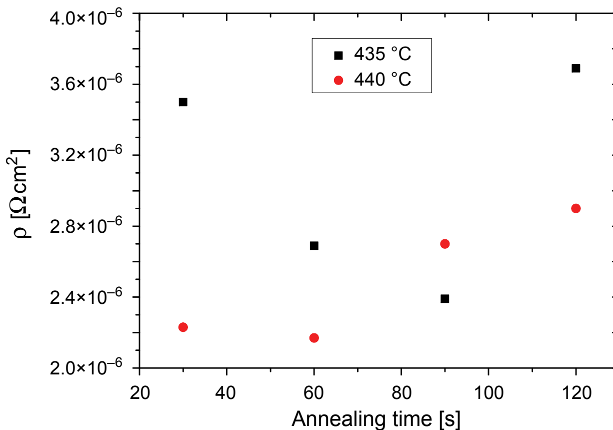


Fig. 3. Specific contact resistance versus annealing time.

The lowest values of the specific contact resistance (about $2\times10^{-6}\ \Omega\,\mathrm{cm}^2$) and good thermal stability were observed for samples annealed for 30 and 60 s at 440 °C and for 90 s at 435 °C. These samples were characterized by good microstructure and smooth surface morphology. For example, the surface morphology of a sample annealed for 60 s at 440 °C is presented in Fig. 4.

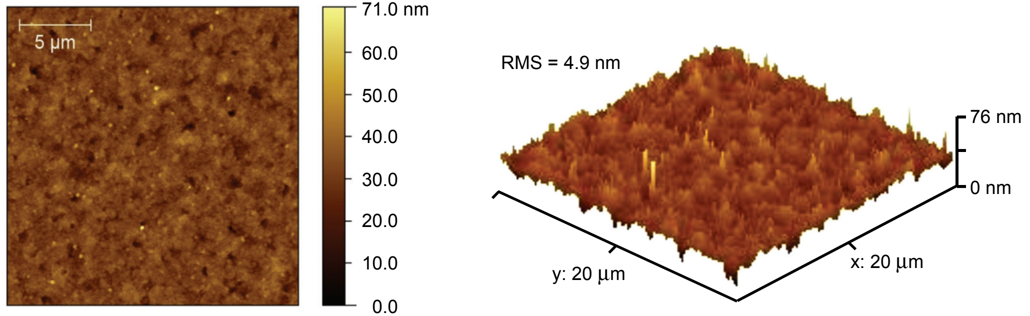


Fig. 4. AFM micrographs (20 µm×20 µm) of surface Ni/AuGe/Ni/Au annealed at 440 °C for 60 s.

The $\beta$-AuGa phase was formed in a relatively uniform layer on the top of the NiAs(Ge) grains and the GaAs:Si substrate. Dark places containing only Au(Ga) phase were observed between the elongated NiAs(Ge) grains.

The second part of this work presents results concerning the AuGe/Ni/Au ohmic contacts. The contact resistance, surface roughness and microstructure studies were performed on samples with different Ni thickness. The contact structure was AuGe(225 nm)/Ni($x$)/Au(300 nm), where $x = 45$ nm (system A), 56 nm (system B), 60 nm (system C), 70 nm (system D), respectively. All samples for the bottom contact (AuGe/Ni/Au system can be used at the bottom of the devices as a contact to GaAs substrate) were annealed at 400 °C for 60 s. The microstructures of the two systems (A – sample with the lowest value of specific resistance, D – sample with the highest value of specific resistance) were compared. The results are shown in Figs. 5 and 6.

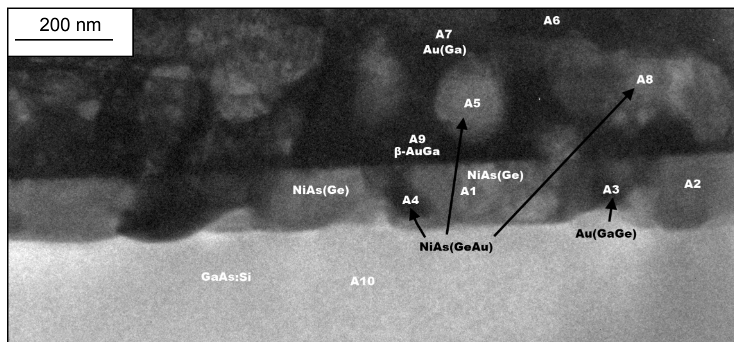


Fig. 5. TEM image of system A – AuGe(225 nm)/Ni(45 nm)/Au(300 nm) after annealing at 400 °C for 60 s.

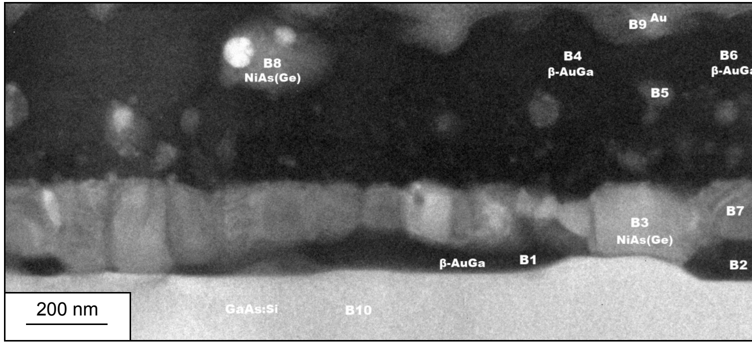


Fig. 6. TEM image of system D – AuGe(225 nm)/Ni(75 nm)/Au(300 nm) after annealing at 400 °C for 60 s.

The results of the EDXS microanalysis performed for these samples are presented in Table 2. The m–s interfaces for system A are composed of uniform NiAs(Ge) grains (location A1, A2 in Fig. 5) and a phase containing mainly Au (location A3, A4 in Fig. 5). About 80% of the total area of GaAs:Si is covered by the NiAs(Ge) grains.

T a b l e 2. Chemical compositions of the phase formed in AuGe/Ni($x$)/Au contacts annealing at 440 °C for 60 s determined by X-ray energy dispersive spectrometry microanalysis.

| Microanalysis location | Thickness of Ni layer [nm] | Chemical composition [at.%] | | | | | Major phase observed |
|---|---|---|---|---|---|---|---|
| | | Ni | Ga | Ge | As | Au | |
| A1 | 45 | 52.85 | 0 | 23.81 | 23.09 | 0.25 | NiAs(Ge) |
| A2 | 45 | 50.54 | 2.21 | 15.73 | 31.32 | 0.20 | NiAs(Ge) |
| A3 | 45 | 7.78 | 8.79 | 2.54 | 5.74 | 75.15 | Au(Ga.Ge) |
| A4 | 45 | 33.63 | 5.85 | 18.75 | 15.02 | 26.75 | NiAs(Ge, Au) |
| A5 | 45 | 37.03 | 2.12 | 14.09 | 21.59 | 25.17 | NiAs(Ge, Au) |
| A6 | 45 | 0 | 10.03 | 0 | 1.68 | 88.29 | Au(Ga) |
| A7 | 45 | 0 | 9.5 | 0 | 2.02 | 88.48 | Au(Ga) |
| A8 | 45 | 40.75 | 0.96 | 17.72 | 22.63 | 17.94 | NiAs(Ge, Au) |
| A9 | 45 | 0 | 11.2 | 0 | 2.69 | 86.11 | $\beta$-AuGa |
| A10 | 45 | 0 | 50.72 | 0 | 49.28 | 0 | GaAs |
| B1 | 75 | 0 | 24.48 | 0 | 3.93 | 71.59 | $\beta$-AuGa |
| B2 | 75 | 0 | 22.65 | 0 | 3.15 | 74.20 | $\beta$-AuGa |
| B3 | 75 | 51.5 | 0 | 3.6 | 44.9 | 0 | NiAs(Ge) |
| B4 | 75 | 0 | 14.83 | 0 | 1.94 | 83.23 | $\beta$-AuGa |
| B5 | 75 | 26.39 | 6.76 | 25.36 | 3.88 | 37.61 | NiAs(Ge, Au) |
| B6 | 75 | 0 | 14.62 | 0 | 1.57 | 83.81 | $\beta$-AuGa |
| B7 | 75 | 51.5 | 0.9 | 4.7 | 42.9 | 0 | NiAs(Ge) |
| B8 | 75 | 51.29 | 0 | 29.46 | 18.87 | 0.38 | NiAs(Ge) |
| B9 | 75 | 0 | 0 | 0 | 2.92 | 97.08 | Au |
| B10 | 75 | 0 | 51.48 | 0 | 48.52 | 0 | GaAs |

T a b l e 3. Experiment results of the AuGe/Ni/Au ohmic contact annealed at 400 °C.

| Ni/AuGe ratio | Annealed for 60 s | | Annealed for 90 s | |
|---|---|---|---|---|
| | Specific resistance [$\times 10^{-6}$ $\Omega$cm$^2$] | Roughness [nm] | Specific resistance [$\times 10^{-6}$ $\Omega$cm$^2$] | Roughness [nm] |
| 0.2 | 1.48 | 8.89 | 2.1 | 5.99 |
| 0.25 | 1.67 | 28.03 | 1.6 | 19.32 |
| 0.27 | 2.18 | 34.21 | 1.98 | 18.43 |
| 0.33 | 2.28 | 49.66 | 4.38 | 43.39 |

The top layer is composed of Au(Ga) phase (location A6, A7 in Fig. 5), $\beta$-AuGa phase (location A9 in Fig. 5) and big NiAs(Ge, Au) grains (location A5, A8 in Fig. 5). On the contrary, the system D has long area of phase containing mainly Au (location B1, and B2) and small portion of NiAs(Ge) phase (location B3) in the m–s interface (Fig. 6). Only about 20% of the total area of GaAs interface is covered by the NiAs(Ge) grains (Fig. 6). A layer composed of $\beta$-AuGa phase and small NiAs(Ge) grains (B5, B8, and B9) was formed on the top of the NiAs(Ge) grains, $\beta$-AuGa layer (location B1 and B2) and GaAs:Si substrate (Fig. 6).

The results for the specific contact resistance and surface roughness are listed in Tab. 3. The surface roughness and specific contact resistance decrease with decreasing thickness of nickel in a barrier layer. The profile measurement gauge micrographs (50 μm×50 μm) of annealed samples at 400 °C for 60 s are shown in Fig. 7. Additionally, the influence of annealing time for GaAs:Si/AuGe/Ni/Au on the morphology and electrical properties is compared.

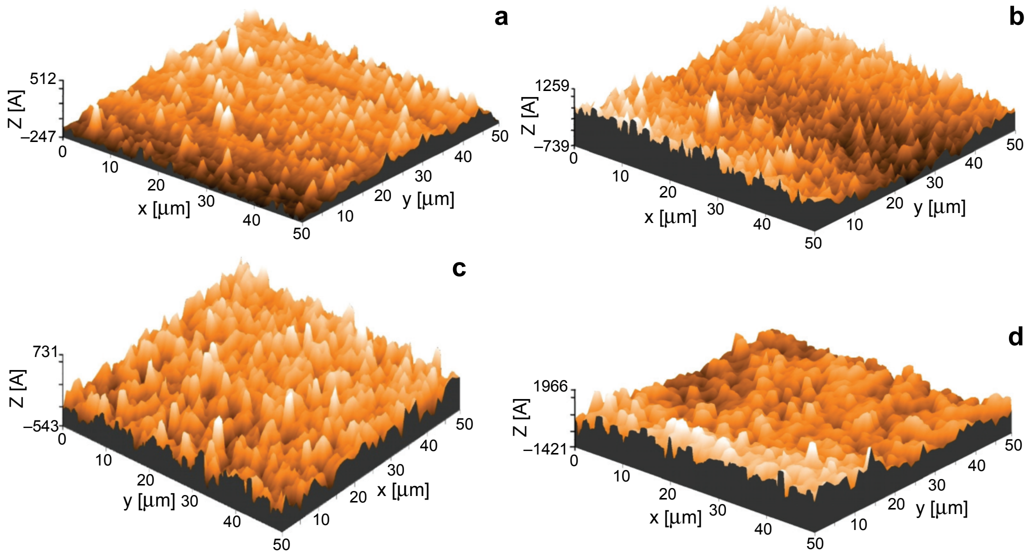


Fig. 7. The micrographs of the surface of AuGe/Ni($x$)/Au contact with $x = 45$ nm (**a**), $x = 56$ nm (**b**), $x = 60$ nm (**c**), and $x = 75$ nm (**d**), annealed at 400 °C, $t = 60$ s.

The lowest values of specific contact resistance (about $1.5\times10^{-6}\ \Omega\mathrm{cm}^2$) and good thermal stability were observed for the samples with the ratio of Ni to AuGe equal to 0.2. These samples were characterized by good microstructure, what means that GaAs:Si surface was covered with lots of NiAs(Ge) grains. The top layer was uniform and consistent with RMS = 8.89 nm.

## 4. Conclusions

Optimal conditions of the technology were determined for two contact systems Ni/AuGe/Ni/Au and AuGe/Ni/Au on the GaAs:Si substrate. For the Ni/AuGe/Ni/Au system the best contact parameters were obtained after annealing at 440 °C for 60 s. The specific contact resistance was $\rho_c = 1.48\times10^{-6}\ \Omega\mathrm{cm}^2$. These samples were characterized by good microstructure (RMS = 4.9 nm) and good thermal stability. The microstructure of this contact was composed of two layers of NiAs(Ge) and $\beta$-AuGa. For the AuGe/Ni/Au system the best contact parameters were obtained where the ratio AuGe/Ni was 0.2 or 0.25. The ohmic contact with this construction after annealing at 400 °C was characterized by low contact resistance $\rho_c = 1.48\times10^{-6}\ \Omega\mathrm{cm}^2$, good morphology with RMS = 9 nm and uniform microstructure composed of two layers of NiAs(Ge) and $\beta$-AuGa. With the increase of the Ni/AuGe ratio the microstructure was deteriorated and NiAs(Ge) grains (responsible for low contact resistance) were displaced from the metal/GaAs interface by the Au-rich phase.

### References

[1] Sirtori C., Nagle J., *Quantum cascade laser: the quantum technology for semiconductor lasers in the mid- far-infrared*, Comptes Rendus Physique **4**(6), 2003, pp. 639–648.

[2] Kosiel K., Szerling A., Bugajski M., Karbownik P., Kubacka-Traczyk J., Sankowska I., Pruszyńska-Karbownik E., Trajnerowicz A., Wójcik-Jedlińska A., Wasiak M., Pierścińska D., Pierściński K., Shubhada Adhi, Ochalski T., Huyet G., *Development of ($\lambda \sim 9.4\ \mu m$) GaAs-based quantum cascade lasers operating at the room temperature*, [In] *Terahertz and Mid Infrared Radiation: Generation, Detection and Applications*, [Eds.] Pereira M.F., Shulika O., NATO Science for Peace and Security Series B: Physics and Biophysics, Springer, 2011, pp. 91–100.

[3] Abhilash T.S, Guruswamy Rajaram, *AuGe–Ni–Au Based Ohmic Contacts to GaAs Structures: Magnetic, Electrical and Morphological Characterization*, LAP Lambert Academic Publishing, 2011.

[4] Murakami M., *Development of refractory ohmic contact materials for gallium arsenide compound semiconductors*, Science and Technology of Advanced Materials **3**(1), 2002, pp. 1–27.

[5] Heiblum M., Nathan M.I., Chang C.A., *Characteristics of AuGeNi ohmic contacts to GaAs*, Solid-State Electronics **25**(3), 1982, pp. 185–195.

[6] Aina O., Katz W., Baliga B.J., Rose K., *Low-temperature sintered AuGe/GsaAs ohmic contact*, Journal of Applied Physics **53**(1), 1982, pp. 777–780.

[7] Yih-Cheng Shih, Murakami M., Wilkie E.L., Callegari A.C., *Effects of interfacial microstructure on uniformity and thermal stability of AuNiGe ohmic contact to* n-*type GaAs*, Journal of Applied Physics **62**(2), 1987, pp. 582–590.

[8] VIDIMARI F., *Improved ohmic properties of Au–Ge contacts to thin* n-*GaAs layers alloyed with an* $SiO_2$ *overlayer*, Electronics Letters **15**(21), 1979, pp. 674–676.

[9] HUNG-CHENG LIN, SENANAYAKE S., KEH-YUNG CHENG, MINGHWEI HONG, KWO J.R., BIN YANG, MANNAERTS J.P., *Optimization of AuGe–Ni–Au ohmic contacts for GaAs MOSFETs*, IEEE Transactions on Electron Devices **50**(4), 2003, pp. 880–885.

[10] REEVES G. K., *Specific contact resistance using a circular transmission line model*, Solid-State Electronics **23**(5), 1980, pp. 487–490.

*Received May 25, 2012*
*in revised form September 30, 2012*